Silicon (2020) 12:1865–1878
https://doi.org/10.1007/s12633-019-00288-1

ORIGINAL PAPER

Simultaneous Removal of Four Dye Pollutants in Mixture Using Amine Functionalized Kit-6 Silica Mesoporous Magnetic Nanocomposite

Shahab Shariati [1] · Abolfazl Chinevari [1] · Mohammad Ghorbani [1]

Received: 26 July 2019 / Accepted: 25 September 2019 / Published online: 11 November 2019
© Springer Nature B.V. 2019

Abstract
In this study, Kit-6 silica mesoporous was created on the surface of magnetite core having silica shell and functionalized by amine group to form Fe3O4@SiO2@Kit-6/NH2 mesoporous magnetic nanocomposites (MMNCs). The synthesized nanocomposite was applied as adsorbent for the removal of four mixed dyes including Sunset Yellow, Rhodamine B, Ponceau 4R and Brilliant Blue from aqueous mixtures. The characterization of the synthesized nanocomposites was investigated by field emission scanning electron microscope (FESEM), transmission electron microscope (TEM), Fourier transform infrared spectroscopy (FT-IR), vibrating sample magnetometry (VSM) and X-ray diffraction (XRD) analysis. N_2 adsorption–desorption method (at 77 K) confirmed the mesoporous structure of synthesized Fe_3O_4@SiO_2@Kit-6/NH_2 MMNCs. The surface area was obtained as 241.68 m^2 g^{-1} (Brunauer- Emmett- Teller, BET method). All of the experimental variables influencing the dyes removal efficiency were investigated using L_{16} Taguchi orthogonal array design. Under optimum conditions (contact time = 20 min, pH = 2, adsorbent weight = 0.08 g (3.2 g L^{-1}) and sample volume = 25 mL); more than 92% of dyes were removed. Adsorption data were studied using Langmuir, Freundlich, and Temkin models to find the best isotherm model. Also, the sorption kinetics were investigated and the best extent of fitting was achieved by the pseudo-second order kinetic model (R^2 = 0.999). The results showed fast kinetics and high removal efficiency of adsorbent, making it as a recoverable adsorbent for removal of these dyes.

Keywords Brilliant blue · Magnetite · Mesopore · Ponceau 4R · Removal · Rhodamine B · Sunset Yellow · Taguchi

1 Introduction

For many years, the process of water purification has been studied because of the presence of various pollutants due to the industrialization of the communities [1]. Dyes are a group of the main water pollutants [2]. Wastewater dyestuffs consume dissolved oxygen during chemical and biological changes. On the other hand, they reduce the amount of sunlight penetration to the depth of water that impacts the photosynthesis reaction and affect the life of the aquatic environment. Also, some of the dye substances and the products derived from their decomposition products are toxic and cancerous. Therefore, treatment of wastewaters is obligatory before their discharge into the environment [3–5].

Up to now, several methods have been improved for the removal of dye substances, including coagulation, membrane separation [6], ultrachemical filtration [7], biological treatment [8], chemical oxidation [9], ion exchange [10], photocatalysis [11] and adsorption [12, 13]. Among these methods, the adsorption process has been extensively considered due to its simple and effective design and ease of operation that is commonly used for removing dyes from aquatic environments. Magnetic nanoscale adsorbents are a new category of adsorbents that have attracted considerable attention in recent years [14–17]. The advantages of magnetic nano-adsorbents, such as low cost and toxicity, high surface area, and easy separation by means of a magnet, provide a great potential for chemical separation. Creation of coatings, as well as the functionalization of the surface of magnetic nanoparticles, is a step taken in improving the quality of adsorption of pollutants from aqueous humor [18–22].

✉ Shahab Shariati
shariaty@iaurasht.ac.ir

[1] Young Researchers and Elite Club, Rasht Branch, Islamic Azad University, Rasht, Iran

In the present research, amine functionalized Kit-6 silica mesoporous magnetic nanocomposites were synthesized. After that, their performance as a recoverable and stable adsorbent for removal of four dye pollutants in the mixture was investigated. According to our knowledge, there is no report on the simultaneous elimination of mixed dyes in the solution. This strategy involves Fe_3O_4 nanoparticle as the magnetic core coated by SiO_2 and after that, Kit-6 mesoporous silica as a layer to form a core/shell structure that is functionalized by amine via post-synthesis method. The synthesized MMNCs were utilized for simultaneous removal of four dye pollutants from aqueous samples.

2 Experimental

2.1 Materials and Chemicals

Sunset Yellow ($C_{16}H_{10}N_2Na_2O_7S_2$, SY), Rhodamine B ($C_{28}H_{31}ClN_2O_3$, RB), Ponceau 4R ($C_{20}H_{11}N_2Na_3O_{10}S_3$, PR), Brilliant Blue ($C_{37}H_{34}N_2Na_2O_9S_3$, BB), ferric chloride hexahydrate ($FeCl_3.6H_2O$), ferrous chloride tetrahydrate ($FeCl_2.4H_2O$), sodium hydroxide (NaOH), ammonia (NH_3, 28 *wt.%*), tetraethyl orthosilicate ($SiC_8H_{20}O_4$, TEOS), 3-aminopropyl triethoxysilane ($C_9H_{23}NO_3Si$, APTES, as organosilane), toluene (C_7H_8), p- toluene sulfonic acid ($CH_3C_6H_4SO_3H$, PTSA), absolute ethanol (C_2H_5OH), 1-butanol ($C_4H_{10}O$) and hydrochloric acid (HCl, 37 *wt.%*) were prepared with adequate purity from Merck (Darmstadt, Germany) and Sigma-Aldrich (Milwaukee, WI, USA). Pluronic P123 (EO_{20}-PO_{70}-EO_{20}, Mw = 5800 g mol^{-1}) was purchased from Sigma-Aldrich. All standard and working solutions were prepared with double distilled water. Figure 1 shows the chemical structures and colors of the four studied dyes in solution.

2.2 Apparatus

XRD pattern of the prepared MMNCs was obtained using X-ray diffraction (XRD) with 2θ range of 0.5-70° on X-PRTPRO (PANalitical, The Netherland). VSM instrument (LBKFB model- Meghnatis Daghigh, Kavir Co., Iran) was applied to investigate the magnetic property of the synthesized nanocomposites. FESEM (MIRA3, TE-SCAN Co., Brno, Czech Republic) was used to study the size and morphology of MMNCs. FT-IR instrument (Shimadzu FT-IR-470, Japan) was used in the wavenumber range of 400-4000 cm^{-1} to study the structural characteristic of the synthesized MMNCs. Energy dispersive X-ray spectroscopy analysis (EDS) was done using a SEM (Sigma VP, ZEISS company, Germany) having EDS detector to show the elemental composition of MMNCs. Nitrogen adsorption-desorption experiments were carried out at 77 K on a Belsorpmini II accelerated surface area and porosimetry system (Bel, Japan). The Brunauer-Emmett-Teller (BET) surface area (S_{BET}) was calculated from the linearity of the BET equation. The surface area, volume and pore diameter of the synthesized MMNCs were calculated from pore size distribution curves using the Barrett Joyner-Halenda (BJH) formula. For spectrophotometric measurements, a Mapada UV-Vis spectrophotometer (6300 PC, China) was used. For magnetic separation, a strong super magnet (1 × 3 × 5 cm) with 1.4 T magnetic field was applied. A Crison pH meter (Basic 20, Spanish) was used for adjusting the pH of solutions.

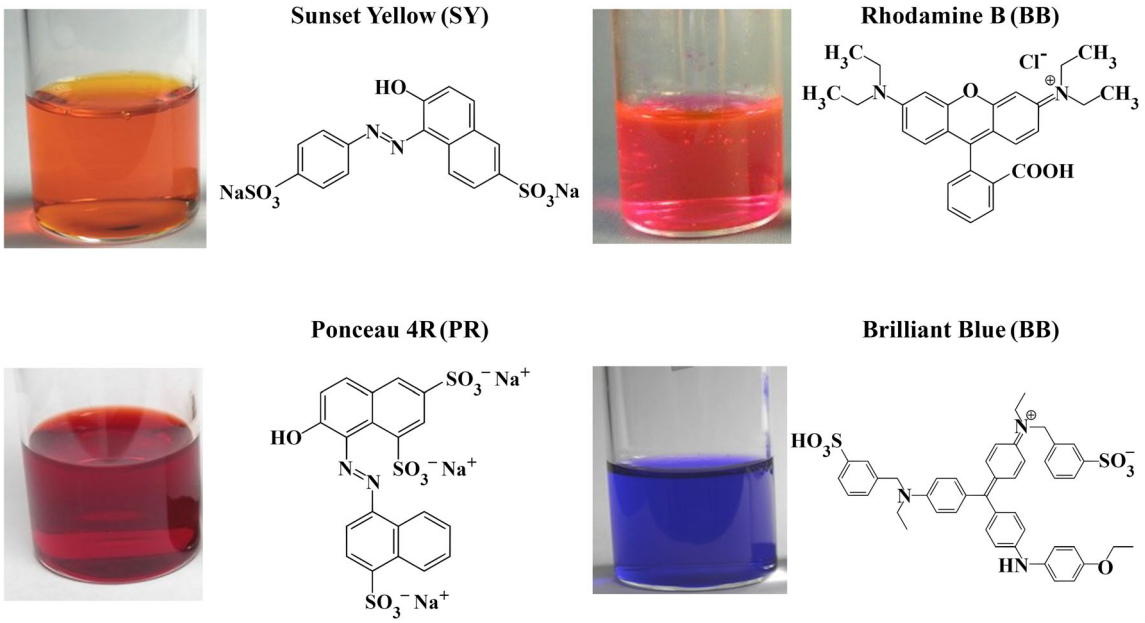

Fig. 1 Chemical structures and colors of Sunset Yellow, Rhodamine B, Ponceau 4R and Brilliant Blue

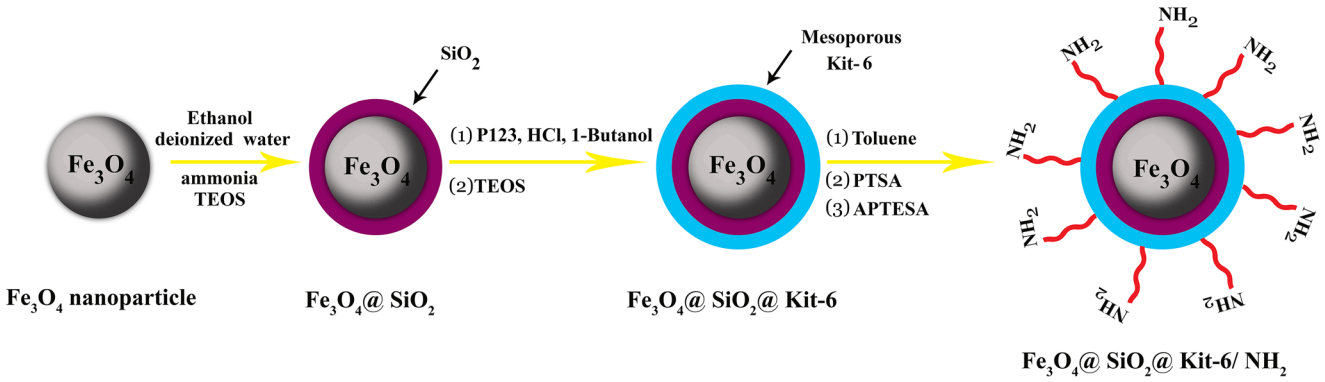

Fig. 2 Schematic for synthesis of Fe_3O_4@SiO_2@Kit-6/NH_2 MMNCs

2.3 Synthesis of Kit-6 Mesoporous Magnetite Nanoparticles Functionalized by Propyl Amine

In the first step, Fe_3O_4 magnetic nanoparticles (MNPs) were synthesized by the chemical precipitation of iron salts in alkaline media. At first, 6.3 g $FeCl_3.6H_2O$, 4.0 g $FeCl_2.4H_2O$ and 3 mL of concentrated hydrochloric acid were added in double distilled water in a 50 mL volumetric flask and the solution was purged with argon gas for 20 min. Then, 250 mL of 1.5 M ammonia solution was added dropwise to the prepared solution at 80 °C under argon gas protection and during vigorous stirring by a magnetic stirrer (1000 rpm). After mixing, MNPs were separated using a super magnet from the solution and were washed four times with double distilled water. Finally, the black magnetite nanoparticles were dried at 90 °C for 4 h [23].

In the second step due to the instability of MNPs under acidic condition used for Kit-6 mesoporous synthesis, a silica layer was coated on the surface of synthesized particles. To create silica shell on the surface of MNPs, 1.0 g of prepared magnetite was suspended in 600 mL ethanol (96%) and the mixture was placed in a water bath for 15 min. Afterward, 20 mL of ammonia (28% *wt.*) was added dropwise at 80 °C and the suspension was stirred vigorously for 15 min. On the other hand, a solution containing 100 mL of ethanol and 10.8 mL of TEOS was slowly added to the initial solution for 2 h. At the end, the nanoparticles of Fe_3O_4@SiO_2 were again separated by the magnet and washed twice with double distilled water. The brown sediments were dried at 90 °C for 3 h.

In the third step, to synthesize the Kit-6 mesoporous structure on the surface of silica-coated magnetite (Fe_3O_4@SiO_2@Kit-6), 1.0 g of Fe_3O_4@SiO_2 nanoparticles was added to a solution containing 1.25 g Pluronic P123, 1.2 mL HCl 37% (*w/w*) and 1.5 mL 1-butanol in 45 mL of double distilled water and the mixture was stirred by magnetic stirrer for 1 h. Afterwards, 2.7 g TEOS was added to the already-prepared mixture and stirred for 24 h. At the end, the mixture was placed in an autoclave for 24 h at 100 °C. The sediment was then washed with double distilled water three times and dried at 90 °C (5 h). Finally, it was placed in a furnace (6 h) to calcify at 550 °C for removal of surfactant residual [23].

In the final step, to functionalize the synthesized nanocomposites, 0.5 g of Fe_3O_4@SiO_2@Kit-6 nanocomposites was initially stirred at 50 °C in 75 mL of toluene (30 min). Then, 3.5 mg PTSA and 2 mg APTES were added to the solution, followed by refluxing at 110 °C (6 h). The MMNCs were separated and washed with ethanol (four times) and then dried at 90 °C (12 h) [24] (Fig. 2).

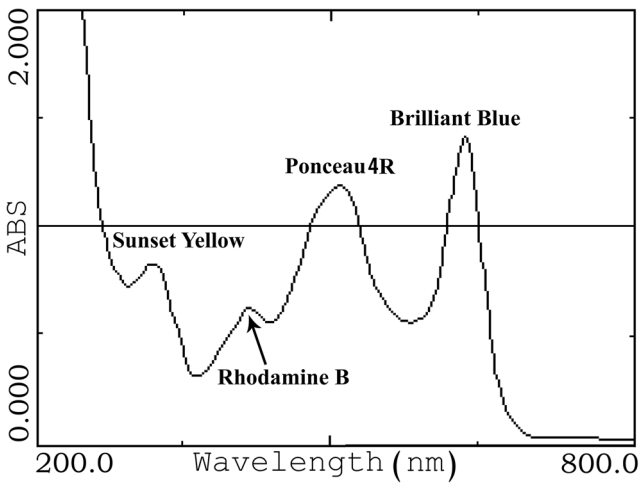

Fig. 3 Absorption spectra for mixture of dyes

2.4 Adsorption Experiments

A mixture solution with 10 mg L^{-1} concentration of each dye pollutant (SY, RB, PR and BB dyes) was prepared from diluting 1000 mg L^{-1} stock solutions of dyes. UV-Vis absorption spectra of each dye as alone and in the mixed solution were obtained using a spectrophotometer and the maximum absorption wavelength was determined for each dye (Fig. 3). According to the spectra, the maximum absorbance wavelengths were obtained as 313, 408, 504 and 628 nm for the SY, RB, PR and BB dyes, respectively. In the following, these

Table 1 Results of the Taguchi experimental design

Number of test	Experimental parameters					Removal efficiency (%)			
	Contact time (min)	pH	Adsorbent weight (g)	Sample volume (mL)	Ionic strength M (NaCl)	SY	RB	PR	BB
1	5	2	0.005	10	0	83.68	76.84	89.88	75.63
2	10	2	0.01	25	0.005	82.36	79.96	90.25	80.97
3	15	2	0.05	50	0.01	93.06	91.39	95.84	93.95
4	20	2	0.08	100	0.05	95.11	92.34	96.04	41.98
5	15	3	0.005	100	0.005	12.78	09.78	14.99	08.06
6	20	3	0.01	50	0	52.10	46.63	55.65	33.10
7	5	3	0.05	25	0.05	74.77	77.40	55.65	96.51
8	10	3	0.08	10	0.01	84.29	78.94	91.61	94.19
9	20	4	0.005	25	0.01	83.76	78.84	90.46	71.76
10	15	4	0.01	10	0.05	35.82	30.85	69.39	93.35
11	10	4	0.05	100	0	60.88	53.25	69.27	39.40
12	5	4	0.08	50	0.005	76.60	71.50	87.71	93.66
13	10	5	0.005	50	0.05	28.84	23.64	33.68	16.10
14	5	5	0.01	100	0.01	23.52	17.75	28.40	07.72
15	20	5	0.05	10	0.005	45.63	35.23	78.79	75.33
16	15	5	0.08	25	0	61.66	54.95	82.82	91.80

wavelengths were used for each dye in all experiments. The mixed standard solutions containing these four dyes in the concentration range of 5-20 mg L^{-1} showed a good linearity (SY: $y = 0.0766\ x - 0.023$, $R^2 = 0.9998$; RB: $y = 0.0507\ x - 0.0175$, $R^2 = 0.9996$; PR: $y = 0.1167\ x - 0.031$, $R^2 = 0.9994$; BB: $y = 0.118\ x - 0.03$, $R^2 = 0.9987$).

In this research, the synthesized MMNCs were applied to remove four mentioned dyes from mixtures. For optimizing the experimental parameters affecting the removal efficiency, Taguchi experimental design method was used. For this purpose, five effective experimental variables including solution pH (2-5), adsorbent weight (0.005-0.08 g), sample volume (10-100 mL), ionic strength (0-0.05 mol L^{-1} NaCl) and contact time (5-20 min) were investigated in four levels [24]. An $OA_{16}(4^5)$ array that represents only 16 experiments, should be performed to complete the optimization process. In the optimization step, all of the experiments were performed randomly with 10 mg L^{-1} of each dye in the mixture. After

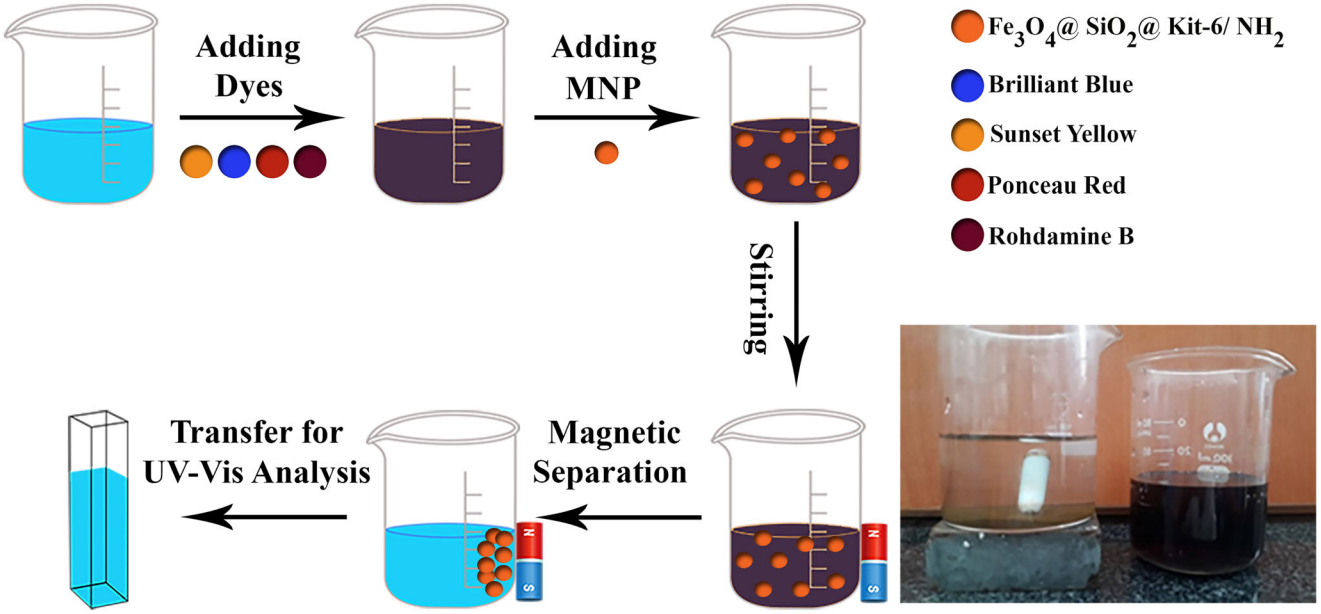

Fig. 4 Removal of mixture of dyes

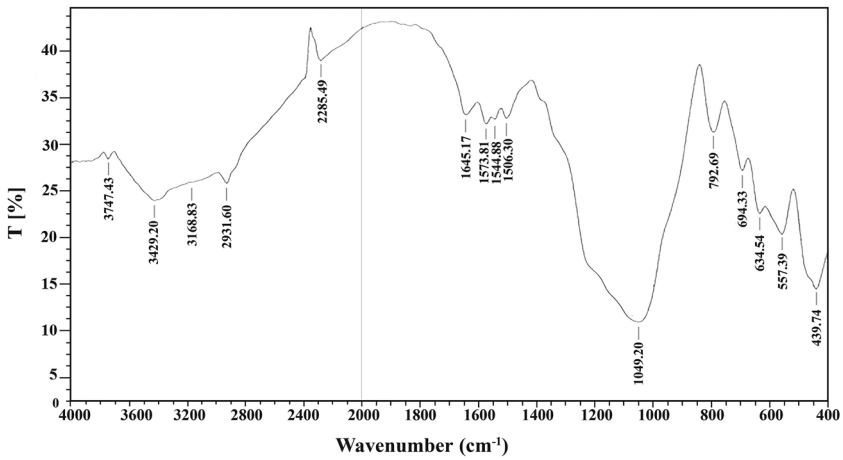

Fig. 5 FT-IR spectra of Fe_3O_4@SiO_2@Kit-6/NH_2

completion of the removal process, the MMNCs were separated from the mixture of dyes with a permanent super magnet. The removal efficiencies were calculated using eq. (1) and the results were shown in Table 1.

Briefly, each adsorption process was carried out as follows: after adjusting the pH of each solution by addition of the appropriate amounts of HCl or NaOH (0.1 mol L^{-1}), the initial absorbance of solution was measured at the wavelength of each dye. Then, a certain amount of synthetic adsorbent was added to the dyes solution. The solution was stirred under optimum conditions for a certain time. At the end of the dye removal process, the adsorbent was separated from the solution by a magnet and the absorbance of the residual solution was measured again (Fig. 4).

Using dye calibration curves, the residual concentration of each dye was calculated in the mixture of dyes and finally, the efficiency of dye removal was obtained using the following equation.

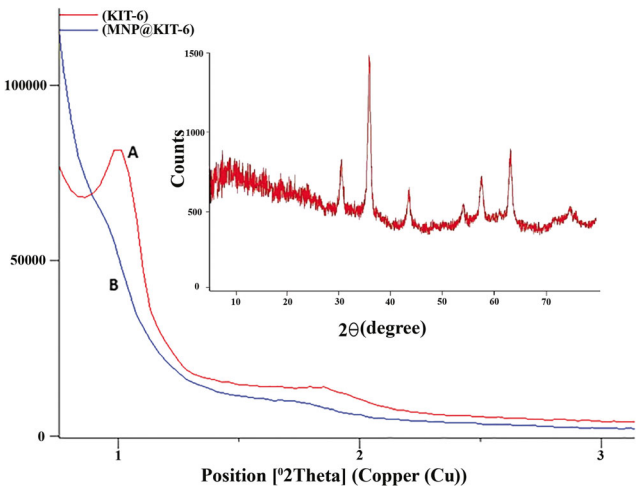

Fig. 6 XRD pattern of mesoporous Kit-6 (red line, A), Fe_3O_4@Kit-6 (blue line, B) in low angels and Fe_3O_4@SiO2@Kit-6 in 2θ range of 10 to 80°

$$Removal\ (\%) = \frac{C_0 - C_t}{C_0} \times 100 \quad (1)$$

Where, C_0 and C_t are the initial and equilibrium concentrations of dyes in the mixture after the adsorption process, respectively.

3 Result and Discussion

3.1 Characterization of the MMNCs

The value of measured magnetization of synthesized Fe_3O_4@SiO_2@Kit-6 nanocomposites was obtained as 15 emu g^{-1} that was lower than the value obtained for pure Fe_3O_4 MNPs (55 emu g^{-1}). This reduction in the magnetization property is due to the coating of pure MNPs with SiO_2 and Kit-6 shells and the shielding effect of silica shell on the core.

FT-IR spectra of MMNCs is shown in Fig. 5. The band in 557.39 cm^{-1} is related to the stretching vibrations of Fe-O bond. This band confirms the presence of iron oxide in the structure of synthesized nanocomposite. Absorption bands observed in the range of 3168.83 cm^{-1} - 3747.43 cm^{-1} are related to the stretching vibrations of -OH groups adsorbed on the surface of Fe_3O_4 nanoparticles.

The observed peaks in 439.74 cm^{-1} and 792.69 cm^{-1} are related to the Si-O-Si symmetric stretching vibrations and the peak in 1049.20 cm^{-1} is related to the Si-O-Si asymmetric stretching vibrations and also the stretching vibrations of Si-OH confirm the presence of silica. The observed peaks in the 1506.30 cm^{-1} to 1654.17 cm^{-1} area are related to the bending vibration of N-H and observed peak in the 3429.20 cm^{-1} is related to the stretching vibration of N-H, which show the mesoporous magnetite surface of the Kit-6 is functionalized by amine groups.

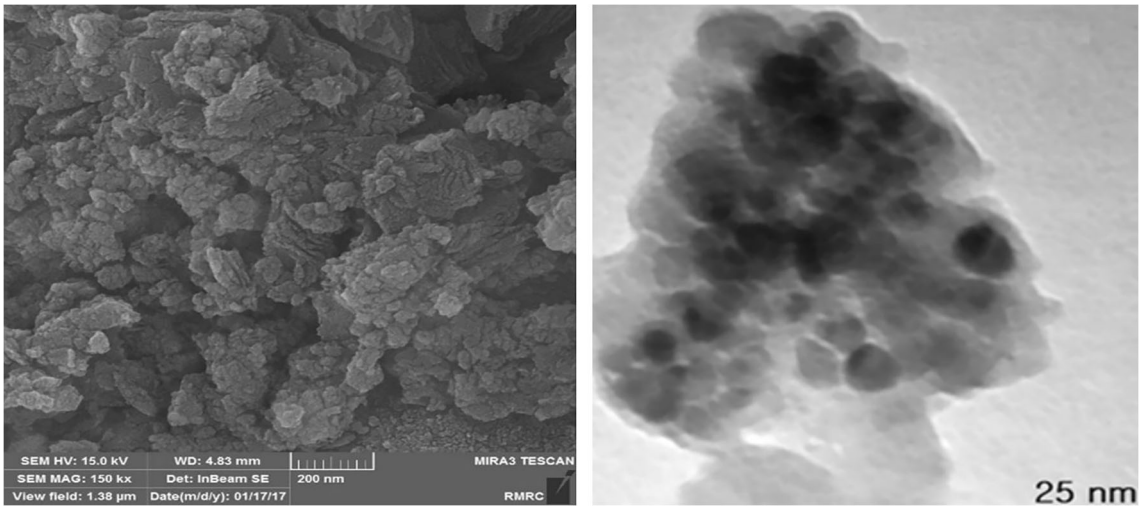

Fig. 7 FESEM (left) and TEM (right) images of Fe_3O_4@SiO_2@Kit-6 nanocomposite

To analyze the crystalline phases of the samples, XRD analysis was performed. As shown in Fig. 6, the XRD pattern shows two reflex angles of 211 and 332 with 2θ at 1° and 1.83° for pure Kit-6, and at 0.89° and 1.76° for the Kit-6 mesoporous magnetite, which confirms the cubic crystal with the space structure (La3d) for the synthetic sample. The reduction in peak intensity of the mesoporous composition is due to the presence of iron nanoparticles, which strongly affect X-ray diffraction. Figure 6c is related to the Kit-6 mesoporous magnetite with 2θ at 4-80°.

The FESEM image of the synthesized Fe_3O_4@SiO_2@Kit-6 nanocomposite shows that the particle size is smaller than 43 nm (Fig. 7). TEM image of the MMNCs is presented in Fig. 7 that shows the magnetic core (dark points) and silica shells (bright point) around them.

The EDS spectra of synthesized Fe_3O_4@SiO_2@Kit-6 NPs confirms the presence of Fe (23.0%), O (51.6%) and Si (25.4%) atoms in the nanocomposite structure (Fig. 8).

Our other studies on the BET and BJH analysis of synthesized nanocomposites confirmed the surface area of 241.68 m^2 g^{-1} and mean pore diameter of 9.25 nm for Fe_3O_4@SiO_2@Kit-6-NH_2 nanocomposites synthesized by this method [24].

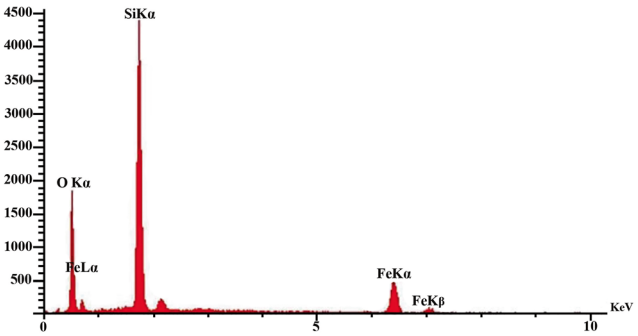

Fig. 8 EDS pattern of synthesized Fe_3O_4@SiO_2@Kit-6 nanocomposite

3.2 Optimization of Experimental Parameters by Taguchi Method

3.2.1 Effects of Stirring Time on the Removal Efficiency of Dyes

As stirring time increases, more opportunity is created for adsorbate to be adsorbed on the adsorbent surface to increase the efficiency of adsorption. Taguchi test method was used in the range of 5-20 min to study the effect of stirring time between the adsorbent and the analyte. The mean removal efficiency of each level of time was calculated and presented in Fig. 9. The results indicate that by increasing the stirring time, the removal efficiency increased for three dyes of SY, RB and PR (Fig. 9, right) and also for the average of four dyes (Fig. 9, left). Therefore, the contact time of 20 min was considered as the optimal time.

3.2.2 Effect of Sample's pH on the Removal Efficiency of Dyes

The pH values of 2, 3, 4 and 5 were investigated in optimization steps. According to the results presented in Fig. 9, it is demonstrated that with a decrease in pH, an increase occurs in the removal efficiency of each dye and the average of dyes. Therefore, pH = 2 is selected as the most suitable pH and the optimal point to obtain the most effective removal.

At the low pHs, the amine groups are protonated and the surface of nanoparticles have a positive charge that facilitates its electrostatic interaction with anionic dyes (Fig. 10).

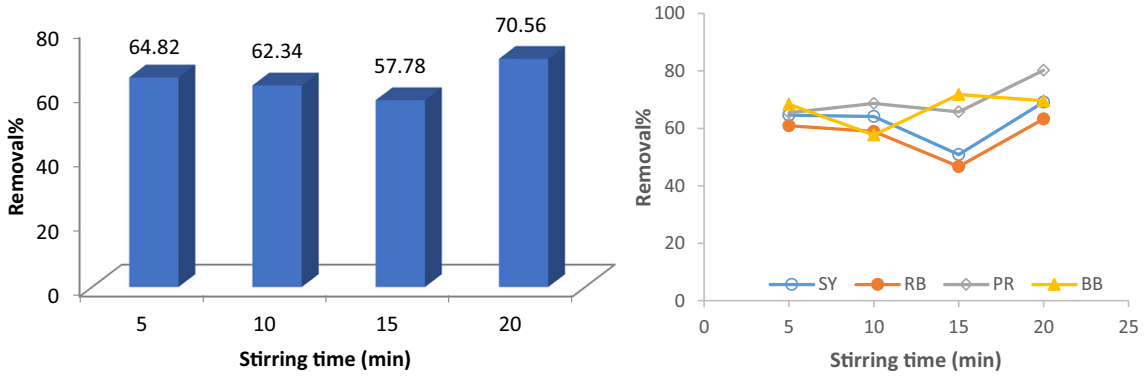

Fig. 9 Effects of stirring time on removal efficiency, (left) average mixture of dyes (right) each dye

3.2.3 Effect of Adsorbent Weight on the Removal Efficiency of Dyes

By increasing the amount of MMNCs in the solution, the active sites for surface adsorption consequently increase, thereby leading to more adsorption. In order to investigate this factor, 0.005, 0.01, 0.05 and 0.08 g of adsorbent were selected in Taguchi test. The results show (Fig. 11) that with an increase in the amount of adsorbent, the adsorption amount of dyes increases on the adsorbent surface (for each dye and the average of dyes) [25]. Therefore, 0.08 g was chosen as the best adsorbent weight for further experiments.

3.2.4 Effect of Sample Volume on the Removal Efficiency of Dyes

For the study of the sample volume, the volumes of 10, 25, 50 and 100 mL of sample were investigated (Fig. 12). According to the average removal efficiency of dyes, the best removal of dyes was obtained for 25 mL of sample solution. Therefore, this value was obtained as the optimum sample volume for further experiments.

3.2.5 Effects of Ionic Strength on the Removal Efficiency of Dyes

When the electrostatic repulsion takes place between the adsorbent surface and analyte, the rise in ionic strength increases the amount of sorption. At the other hands, when electrostatic attraction exists, the increase in ionic strength reduces the analyte adsorption on the adsorbent surface.

To evaluate the effect of ionic strength of the solution, sodium chloride (NaCl) was used at concentrations of 0, 0.005, 0.01 and 0.05 mol L^{-1}. According to the results (Fig. 13), the increase in ionic strength reduces the amount of adsorbing dyes on the surface. Consequently, in optimal conditions, experiments were carried out with no salt addition. The presence of high concentrations of salt, prevents the proper interaction of dye with the adsorbent by forming a coating layer on the surface of magnetic nanoparticles.

3.2.6 Evaluation of Removal Efficiency at Optimum Conditions

To evaluate the removal efficiency of the dyes mixtures under optimal experimental conditions obtained by Taguchi experimental design (contact time = 20 min, pH = 2, adsorbent

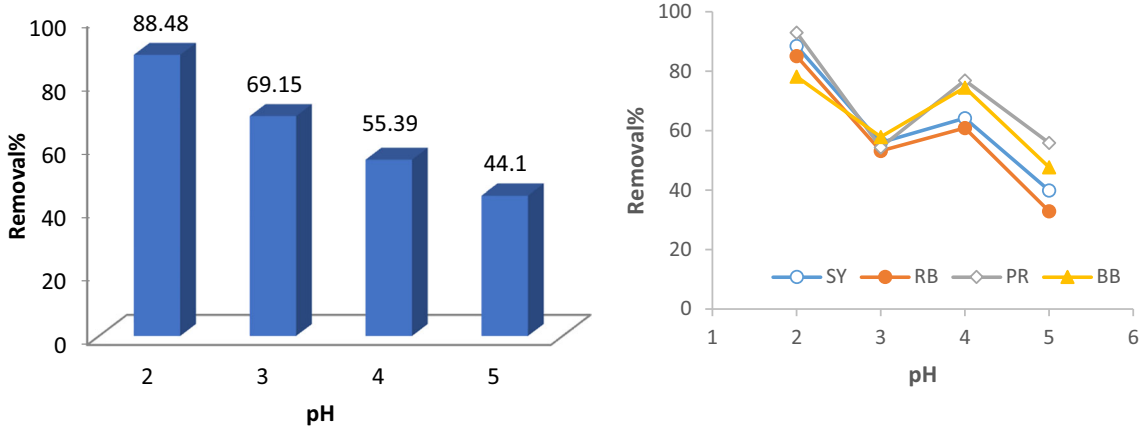

Fig. 10 Effect of sample's pH on removal efficiency, (left) average mixture of dyes (right) each dye

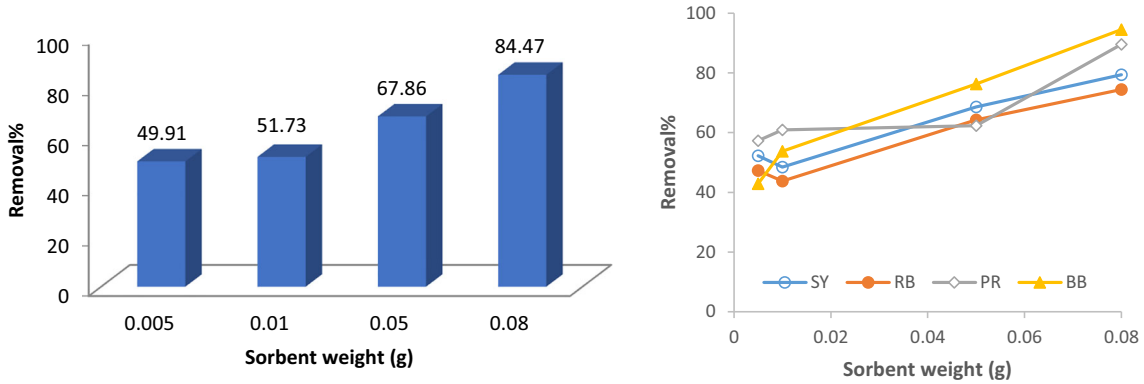

Fig. 11 Effect of adsorbent weight on removal efficiency, (left) average mixture of dyes (right) each dye

weight = 0.08 g (3.2 g L^{-1}) and sample volume = 25 mL), a mixture solution was prepared with the concentration of 10 mg L^{-1} of each dye. The solution was acted under the optimal condition and after removal by the adsorbent, the removal efficiencies were measured in optimum conditions. The dye removal process was repeated for three times under optimal conditions and the results indicated 92% removal of mixed dyes in the solution.

3.3 Adsorption Isotherm

For better understanding the interactions between adsorbate and adsorbent, in the present study, Langmuir, Freundlich and Temkin isotherms were investigated.

To study of isotherms, concentrations of dyes were adjusted in the range of 2 - 20 mg L^{-1} and the experiments were performed under optimum conditions. The results are presented in Figs. 14, 15 and 16 and Table 3.

Langmuir isotherm that is applicable for homogenous surface adsorption is shown in Eq. 2.

$$\frac{C_e}{Q_e} = \frac{1}{k_L\, q_m} + \frac{C_e}{q_m} \tag{2}$$

Where C_e and Q_e are the equilibrium concentration of the dye solution (mg L^{-1}) and the amount of adsorbed dye per mass of adsorbent (mg g^{-1}), respectively. q_m is the maximum adsorption capacity (mg g^{-1}) and k_L is the Langmuir constant, which is related to the adsorption energy (L mg^{-1}) [26].

The Freundlich isotherm that is derived assuming heterogeneity surface with its adsorption sites at changeable energy levels, is obtained from the following Eq. 3.

$$\mathrm{Log}q_e = \log(k_f) + \frac{1}{n}\log(C_e) \tag{3}$$

Where q_e is the amount of adsorbed dye in equilibrium condition (mg g^{-1}), k_f ($mg^{1-(1/n)}\ L^{1/n}\ g^{-1}$) is the Freundlich constant and n is the heterogeneity factor [27–28]. k_f and n indicate the adsorption capacity and the adsorption intensity, respectively. If the value of $1/n$ is lower than 1, it defines a normal Freundlich isotherm; if not, it is indicative of cooperative adsorption.

Temkin isotherm contains a factor that is taking into the account of adsorbent-adsorbate interactions. By ignoring the extremely low and large value of concentrations, the model assumes that heat of adsorption of all molecules in the layer would decrease linearly with the surface coverage. This model can be presented by the Eq. 4.

$$q_e = k_1 \mathrm{Ln}(k_2) + k_1 \mathrm{Ln}(C_e) \tag{4}$$

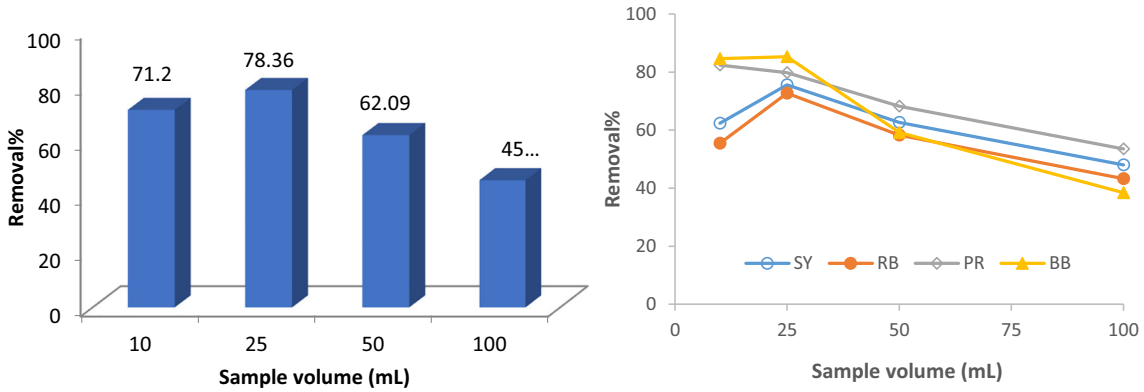

Fig. 12 Effect of sample volume on removal efficiency, (left) average mixture of dyes (right) each dye

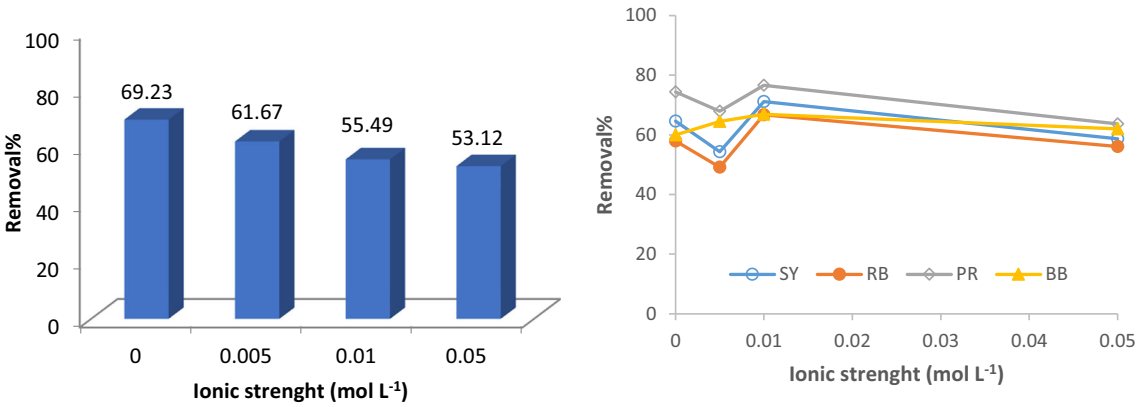

Fig. 13 Effects of ionic strength on removal efficiency, (left) average mixture of dyes (right) each dye

Fig. 14 Langmuir isotherm to remove mixture of dyes and each dye

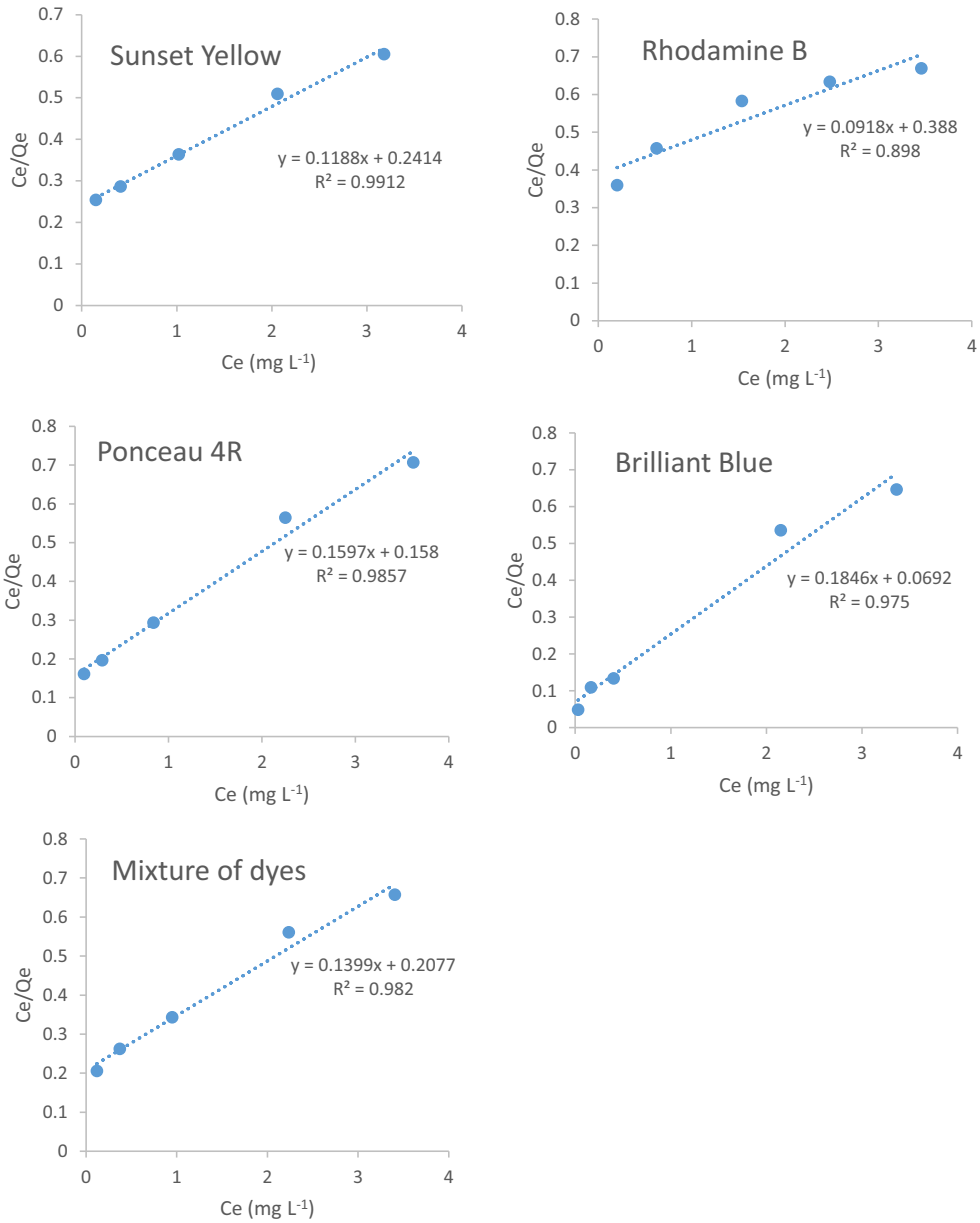

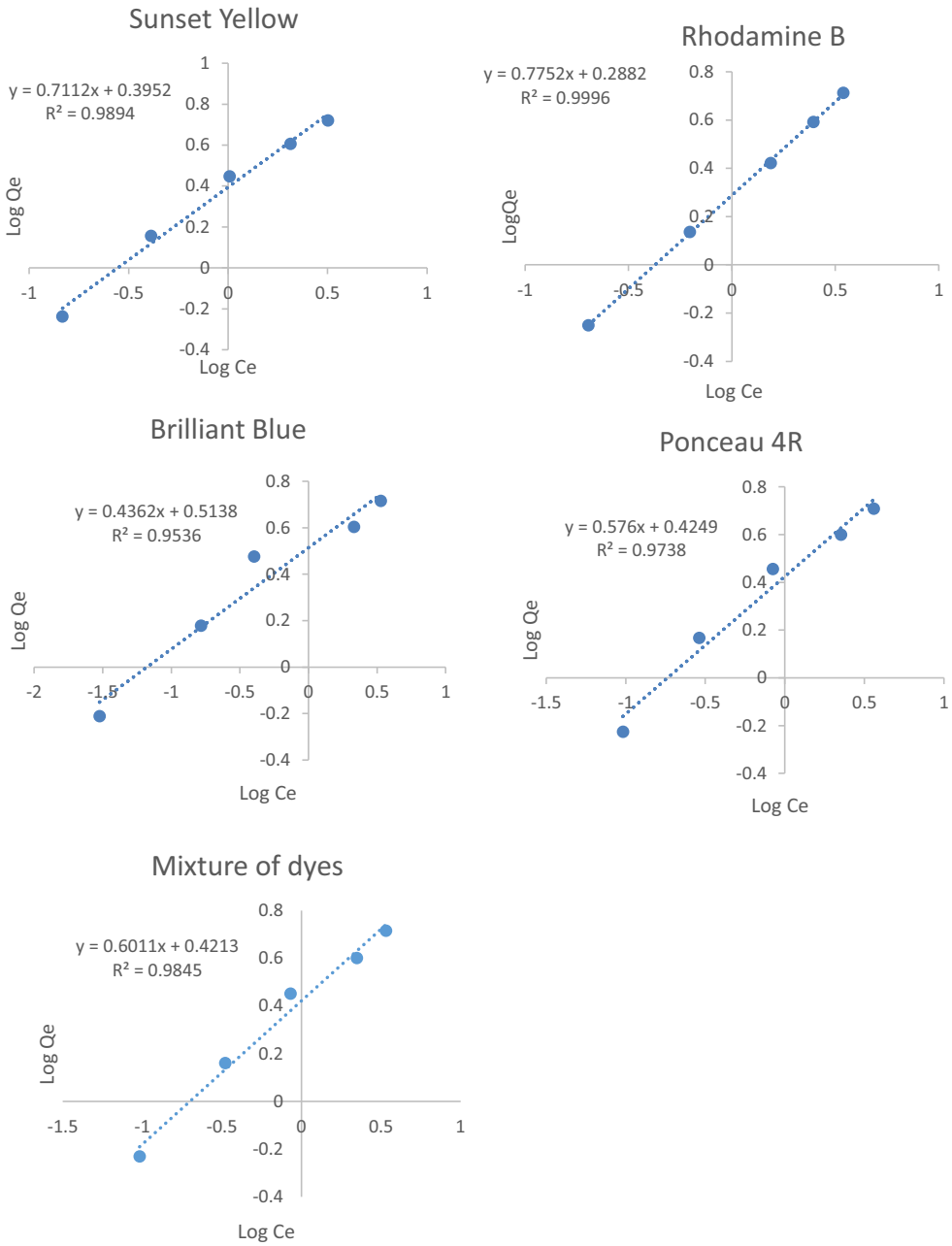

Fig. 15 Freundlich isotherm to remove mixture of dyes and each dye

Where k_1 is Temkin isotherm equilibrium constant (L g^{-1}), which is related to the heat of sorption (J mol^{-1}) and k_2 is Temkin isotherm constant [29].

The constant parameters of all four models for each dye (alone and in mixture of dyes) are listed in Table 2. The adsorption of SY, PR and BB dyes shows better fitting to the Langmuir isotherm model rather than two other models. The higher correlation coefficient (R^2= 0.9912 for SY; 0.9857 for PR and 0.9750 for BB) of Langmuir isotherm refers to monolayer adsorption of these dyes on the surface of nanocomposites. For adsorption of RB dye, the correlation coefficients show that Freundlich isotherm was better fitted to isotherm data than Langmuir or Temkin isotherms (R^2 = 0.9996). The adsorption is suitable when the Freundlich constant (n) takes values within the range of 1–10. In this study, n value of 1.0786 shows the satisfactory adsorption.

Also, to evaluate the favorability of the adsorption process, the dimensionless separation factor (R_L) was calculated using the following equation:

$$R_L = \frac{1}{1 + k_1 C_0} \tag{5}$$

The adsorption process can be defined as favorable (0 <R_L< 1), unfavorable (1 < R_L), linear (R_L = 1) and irreversible in nature (R_L = 0) [30]. In this study, the value of R_L calculated

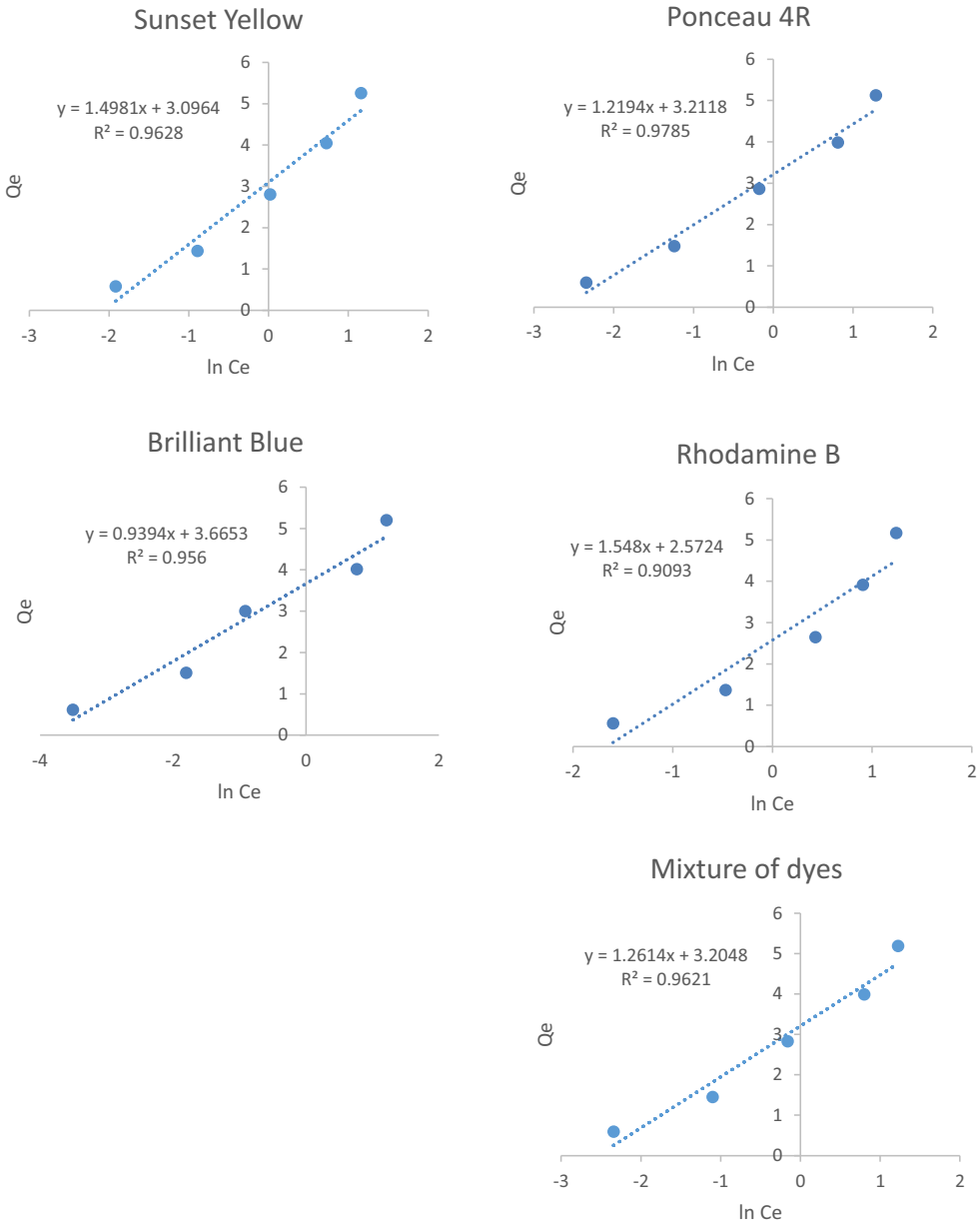

Fig. 16 Temkin isotherm to remove mixture of dyes and each dye

Table 2 The obtained parameters of isotherm models

Adsorption isotherm	Langmuir				Freundlich			Temkin		
Parameter	q_m	K_l	R^2	R_L	K_f	n	R^2	K_t	K_l	R^2
SY	08.41	0.492	0.9912	0.1689	2.484	1.406	0.9894	1.498	7.899	0.9628
RB	10.89	0.236	0.8980	0.2976	1.941	1.289	0.9996	1.548	5.268	0.9093
PR	06.26	1.010	0.9857	0.0908	2.660	1.736	0.9738	1.219	13.927	0.9785
BB	05.41	2.667	0.9750	0.0361	3.264	2.292	0.9536	0.939	49.486	0.9560
Mixture of dyes	07.14	0.0673	0.9820	0.5977	2.638	1.663	0.9845	1.261	12.687	0.9621

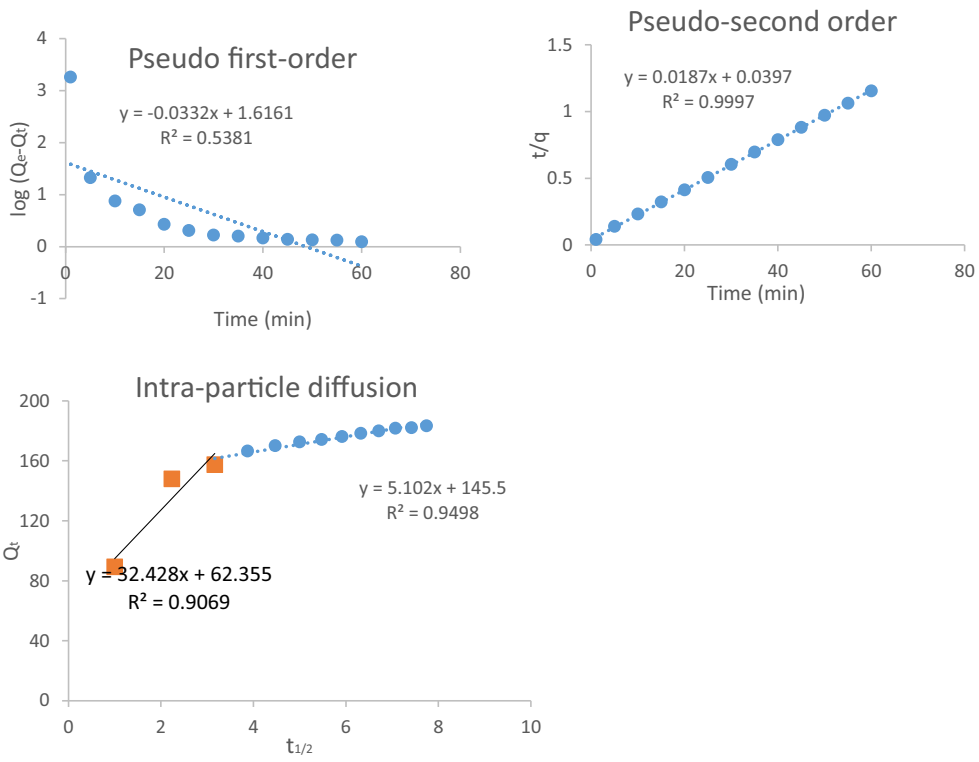

Fig. 17 Adsorption kinetics for removal mixture of mixture of dyes

for the adsorption of dyes ($[dye]_0 = 10$ mg L^{-1}) by Fe_3O_4@SiO_2@Kit-6/NH_2 MMNCs fall between 0 and 1 [31]. Therefore, the adsorption of these dyes onto the adsorbent appears to be a favorable process.

3.4 Adsorption Kinetics

For the kinetics studies of the dyes removal process by MMNCs, the experiments were carried out in optimal conditions and in the time range of 0 to 60 min. Pseudo First-order, pseudo second-order and intra-particle diffusion models were investigated to study the adsorbent behavior and adsorption process mechanism. The results are presented in Fig. 17 and Table 3.

The pseudo first-order kinetic model is obtained from Eq. 6.

$$\log(q_e - q_t) = \log q_e - \frac{k_1.t}{2.303} \quad (6)$$

Which q_e and q_t are the amount of adsorbed dye (mg g^{-1}) at equilibrium time and at the time t, respectively. k_1 (min^{-1}) is the pseudo first-order rate constant. The values of k_1 and q_e are calculated from the slope and intercept of the plot of log ($q_e - q_t$)versus t, respectively.

The kinetic rate equation for pseudo-second order reaction model can be written as follows (Eq. 7):

$$\frac{t}{q_t} = \frac{1}{k_2 q_e^2} + \left(\frac{1}{q_e}\right)t \quad (7)$$

Where q_t and q_e, are the values of adsorbed dye at each time and at equilibrium and k_2 (g mg^{-1} min^{-1}) is the pseudo-second order rate constant. The second-order rate constant (k_2) can be obtained from the slope and intercept of the plot of $\frac{t}{q_t}$ versus t, respectively.

Also, intra-particle diffusion resistance influencing the adsorption process was investigated, whose related equation is given as:

$$q_t = k_{diff} t^{\frac{1}{2}} + C \quad (8)$$

Where k_{diff} (mg g^{-1} $min^{-1/2}$) is the intra-particle diffusion rate constant which can be evaluated from the slope of the linear plot of q_t versus $t^{1/2}$ and C (mg g^{-1}) is the thickness of the boundary layer. Value of C is related to the thickness of the

Table 3 The obtained parameters of kinetic models

Kinetic model	Pseudo first-order			Pseudo second-order			Intra-particle diffusion		
Parameter	q_e	k_1	R^2	q_e	k_2	R^2	k	C	R^2
	41.314	−0.076	0.5380	53.47	0.008	0.9997	10.47	112.66	0.7392

boundary layer. The effect of the boundary layer is greater when C gets larger.

The results indicated fast dye adsorption on the surface of the mesoporous magnetite surface which corresponds to the pseudo second-order kinetic model and represents a chemical adsorption mechanism. Regarding the high regression coefficient of the pseudo second-order kinetic model (R^2= 0.9997), the kinetic of dyes adsorption process is best described by this model.

This result shows that chemical reaction appears during adsorption of dyes on the surface of MMNCs. For the intra-particle diffusion model, the value of C was obtained as 112.66 mg g^{-1} ($C \neq 0$). This result indicates that intra-particle diffusion is not the only rate limiting step for adsorption. The sorption process is rather complex and involves more than one diffusive resistance.

3.5 Reusability Studies of Adsorbent

To investigate the adsorption capability during several stages of reuse, after each step, the adsorption process was carried out and the adsorbent was removed from the adsorbent surface and after dye desorption and drying, re-adsorption was permitted. Desorption experiments were performed using 10 mL of 0.1 mol L^{-1} NaOH for 10 min and the dye molecules were completely desorbed. The results show the high adsorbent ability to be reused for removal of dyes (more than 80% removal after 5 adsorption cycles).

4 Conclusion

The results of this study indicated the surface of the synthesized magnetic nanocomposite was not limited to adsorb a specific dye. It was possible for such nanocomposites to simultaneously eliminate several dyes with a high adsorption capacity through an electrostatic attraction between the amine functional groups of MMNCs and dyes. The fast and easy magnetic separation of nanocomposites using an external magnetic field after adsorption process, as well as high adsorption capacity, reusability, rapid sorption kinetics and simultaneous adsorption of different dyes are the advantages of the proposed adsorbent.

Acknowledgements The authors are grateful to Young Researchers and Elite Club, Rasht Branch, Islamic Azad University for their support.

References

1. Zhao L, Chi Y, Yuan Q, Li N, Yan W, Li X (2013) Phosphotungstic acid anchored to amino–functionalized core–shell magnetc mesoporous silica microspheres: A magnetically recoverable nanocomposite with enhanced photocatalytic activity. J Colloid Interface Sci 390:70–77
2. Peng L, Qina P, Lei M, Zeng Q, Song H, Shao J, Liao B, Gu J (2012) Modifying Fe_3O_4 nanoparticles with humic acid for removal of Rhodamine B in water. J Hazard Mater 209–210:193–198
3. Ghaedi M, Pakniat M, Mahmoudi Z, Hajati S, Sahraei R, Daneshfar A (2014) Synthesis of nickel sulfide nanoparticles loaded on activated carbon as a novel adsorbent for the competitive removal of Methylene blue and Safranin-O. Spectrochim Acta A 123:402–409
4. Baskaralingam P, Pulikesi M, Elango D, Ramamurthi V, Sivanesan S (2006) Adsorption of acid dye onto organobentonite. J Hazard Mater 128:138–144
5. Seyed Danesh SM, Faghihian H, Shariati S (2019) Sulfonic Acid Functionalized SBA-3 Silica Mesoporous Magnetite Nanocomposite for Safranin O Dye Removal. Silicon. 11:1817–1827
6. Gürses A, Doğar Ç, Yalçın M, Açıkyıldız M, Bayrak R, Karaca S (2006) The adsorption kinetics of the cationic dye, methylene blue, onto clay. J Hazard Mater 131:217–228
7. Allègre C, Moulin P, Maisseu M, Charbit F (2006) Treatment and reuse of reactive dyeing effluents. J Membr Sci 269:15–34
8. Kornaros M, Lyberatos G (2006) Biological treatment of wastewaters from a dye manufacturing company using a trickling filter. J Hazard Mater 136:95–102
9. Dutta K, Mukhopadhyaya S, Bhattacharjee S, Chaudhuri B (2001) Chemical oxidation of methylene blue using a Fenton-like reaction. J Hazard Mater 84:57–71
10. Liu CH, Wu JS, Chiu HC, Suen SY, Chu KH (2007) Removal of anionic reactive dyes from water using anion exchange membranes as adsorbers. Water Res 41:1491–1500
11. Muruganandham M, Swaminathan M (2006) TiO_2–UV photocatalytic oxidation of reactive yellow 14: effect of operational parameters. J Hazard Mater 135:78–86
12. Deligeer W, Gao YW, Asuha S (2011) Adsorption of methyl orange on mesoporous Fe_2O_3/SiO_2 nanocomposites. Appl Surf Sci 257: 3524–3528
13. Toutounchi S, Shariati S, Mahanpoor K (2019) Sulfonic acid functionalized magnetite nanomesoporous carbons for removal of Safranin O from aqueous solutions. Desalin Water Treat 153:253–263
14. Shariati S, Mokhtary M (2018) Modified magnetic nanoparticles for the removal of organic pollutants. LAP LAMBERT Academic Publishing
15. Tang SCN, Lo IMC (2013) Magnetic nanoparticles: Essential factors for sustainable environmental applications. Water Res 47 (8: 2613–2632
16. Kefeni KK, Mamba BB, Msagati TAM (2017) Application of spinel ferrite nanoparticles in water and wastewater treatment: A review. Sep Purif Technol 188:399–422
17. Kaili Q, Weijun T, Jie B, Liang W, Jing Z, Zhaoyang D, Xiaoxi G (2019) Application of magnetic adsorbents based on iron oxide nanoparticles for oil spill remediation: A review. J Taiwan Inst Chem E 97:227–236
18. Jiang Z, Xie J, Jiang D, Yan Z, Jing J, Liu D (2014) Enhanced adsorption of hydroxyl contained/anionic dyes on non functionalized Ni@SiO_2 core–shell nanoparticles: Kinetic and Thermodynamic profile. Appl Surf Sci 292:301–310
19. Zhang X, Niu H, Pan Y, Shi Y (2011) Y Cai, Modifying the surface of Fe_3O_4/SiO_2 magnetic nanoparticles with C_{18}/NH_2 mixed group to get an efficient sorbent for anionic organic pollutants. J Colloid Interface Sci 362:107–112
20. Sojoudi M, Shariati S, Khabazipour M (2016) Amine functionalized Kit-6 mesoporous magnetite nanocomposite as an efficient adsorbent for removal of Ponceau 4R dye from aqueous solutions. Anal Bioanal Chem Res 3:287–298

21. Seyed Danesh SM, Faghihian H, Shariati S (2018) Sulfonic acid functionalized magnetite nanoporous-KIT-6 for removal of methyl green from aqueous solutions. J Nanopart Res 52:54–70
22. Toutounchi S, Shariati S, Mahanpoor K (2019) Synthesis of nano-sized magnetite mesoporous carbon for removal of Reactive Yellow dye from aqueous solutions. Appl Organomet Chem. https://doi.org/10.1002/aoc.5046
23. Shariati S, Khabazipour M, Safa F (2017) Synthesis and application of amine functionalized silica mesoporous magnetite nanoparticles for removal of chromium (VI) from aqueous solutions. J Porous Mater 24:129–139
24. Khabazipour M, Shariati S, Safa F (2016) SBA and KIT-6 mesoporous silica magnetite nanoparticles: synthesis and characterization. Synth React Inorg Met Org Chem 46:759–765
25. Keyhanian F, Shariati S, Faraji M, Hesabi M (2016) Magnetite nanoparticles with surface modification for removal of methyl violet from aqueous solutions. Arab J Chem 9:348–354
26. Langmuir I (1916) The constitution and fundamental properties of solids and liquids. Part I. solids. J Am Chem Soc 38:2221–2295
27. Hanafiah MAKM, Ngah WSW, Zolkafly SH, Teong LC, Majid ZAA (2012). J Environ Sci 24:261–268
28. H. Freundlich, W. Engelmann. 1906
29. Temkin MI, Pyzhev V (1940) Kinetic of Ammonia Synthesis on Promoted Iron Catalyst. Acta PhysChim USSR 12:327–356
30. Mohammadi Galangash M, Niyazi Kolkasaraei Z, Ghavidast A, Shirzad-Siboni M (2016) Facile synthesis of methyl propylaminopropanoate functionalized magnetic nanoparticles for removal of acid red 114 from aqueous solution. RSC Adv 6: 113492–113502
31. Mohammadi Galangash M, Ghavidast A, Bozorgpanah Z (2019) Adsorption of acid red 114 and reactive black 5 in aqueous solutions on dendrimer-conjugated magnetic nanoparticles. J Chin Chem Soc 66(1):62–74

Publisher's Note Springer Nature remains neutral with regard to jurisdictional claims in published maps and institutional affiliations.